ELUCIDATION OF THE FRONTIER ORBITALS OF BENZENE DERIVATIVES BY COMPUTATIONAL AND THEORETICAL CHEMISTRY

Michael Arfanis*, Iuliia Mileeva*, Hua Deng and Chwen-Yang Shew†

Department of Chemistry, College of Staten Island, Staten Island, NY 10314

Abstract

Density function theory (DFT) and time-dependent density functional (TD-DFT) theory are essential tools in elucidating molecular structures and orbitals. These methods were applied to calculate the frontier orbitals, HOMO and LUMO, of three series of benzene derivatives including C_6H_5-XH_3, X = C, Si, Ge; C_6H_5-YH_2, Y = N, P, As; and C_6H_5-ZH, Z = O, S, Se. The calculated results were compared with Hückel theory which showed that DFT and TD-DFT differ mainly in their calculations of π-bonding resonance integrals. The HOMO-LUMO gap of benzene derivatives displayed red shifts in both computational methods. The calculated energy gaps for both methods were moderately correlated with the electronegativity of the non-hydrogen element in the substituent group. A locally modified Hückel theory fitted the HOMO and LUMO energies of C_6H_5-ZH derivatives well. The difficulties in extending Hückel theory to quantify the other series suggested that global bonding modifications are needed among those molecules.

†Corresponding author:ChwenYang.Shew@csi.cuny.edu *Undergraduate researchers and co-authors
Keywords: Computational Chemistry; DFT; TD-DFT; Hückel Theory; Benzene Derivatives; Frontier Orbitals; Molecular Structure
Received: August 25, 2025 Accepted: September 23, 2025 Revision Received: September 27, 2025 Published: October 1, 2025

Introduction

Computational quantum chemistry has become a standard numerical tool for chemical research.[1] Besides molecular geometry, quantum calculations predict the frontier molecular orbitals including HOMO (highest occupied molecular orbital) and LUMO (lowest unoccupied molecular orbital). These frontier orbitals are important intrinsic properties of molecules relevant to their photophysics, photochemistry, reactivity, acidity, basicity, redox reactions, and so on.[2]

A variety of quantum chemistry methods have been developed over the past decades. Density functional theory (DFT) by Kohn and Sham has become one of the widely studied and tested methods, which takes electron-electron correlation into account in the calculation.[3,4] The DFT often predicts accurate molecular structures that links with the ground electronic states of a molecule and can be more effective at dealing with larger molecules.[5]

Despite the advancement of DFT in studies of molecular structures at ground state, its predictions of LUMO need to be cross-examined. To address such an issue, time-dependent density functional theory (TD-DFT) was developed.[6] The TD-DFT stresses electronic transitions and can be used to calculate the UV-VIS spectroscopy of a molecule, for example.[7] Therefore, TD-DFT produces more reliable molecular orbitals, including LUMO.[7,8]

This work first applied DFT and TD-DFT to investigate three series of benzene derivatives: (1) $C_6H_5XH_3$ with X = C, Si , Ge; (2) $C_6H_5YH_2$ with Y = N, P, As; (3) $C_6H_5ZH_2$ with Z = O, S, Se, as shown in Figure 1. These derivatives find applications in numerous industries, such as pharmaceutical drug designs, manufacture of polymers and plastic materials, industrial solvents, and pigments.[9,10] Moreover, a substituent group on benzene dictates the position of the second substituent group on a benzene ring.[11] The above benzene derivatives are ideal candidates that can be studied by using Hückel theory.[12]

Hückel theory was developed to simplify the complex quantum chemistry calculation for the planar conjugate molecules.[12] In Hückel theory, there are two fundamental quantities: Coulomb integral α and resonance integral β.[13] Coulomb integral is related to local interactions between an electron and a nucleus prior to bond formation. Resonance integral arises from quantum effects and is often viewed as the hopping of an electron between two neighboring nuclei. The resonance integral accounts for the energy gain of bond formation.[13]

Some modifications of Hückel theory have been extended to investigate heterocyclic compounds and the benzene derivatives with single substituents.[14] The schematic of the model is shown in Figure 1. The Hückel theory was adapted to compare with the HOMO and LUMO energies and the HOMO-LUMO gaps calculated from DFT and TD-DFT for the derivatives in Figure 1. Also this work explored the possibility of applying Hückel theory to explain the computational results.

Computational Methods

Computational Quantum Chemistry Methods

A thorough computation chemistry calculation was conducted to compare the HOMO and LUMO states of benzene and its 9 different derivatives in Figure 1. The ORCA 6.0 computational chemistry package was applied for the required calculations.[15] This package comes with DFT and TD-DFT which provides predictions for the molecular geometry and frontier orbitals of a molecule.

The calculation was started with geometry optimization by using the highly recommended density functional theory B3LYP with the 6-311++g(d,p) basis set.[16] This choice was known for its accuracy and short computational time to determine the ground state properties of a molecule, like molecular structure. Nevertheless, its predictions of LUMO states need to be checked with other methods.[7] Since B3LYP is not the best functional for TD-DFT calculations, we resorted to the ωB97X-D3 functional with the basis set def2-TZVP in TD-DFT calculations. [17] The TD-DFT

with ωB97X-D3 is capable of computing the UV-VIS spectrum of a molecule and is expected to better predict both HOMO and LUOM states.[17] However, ωB97X-D3 is a much more expensive method than B3LYP in computation during our test with aniline. In the test, the optimal conformations resulting from B3LYP and ωB97X-D were very close. As such, we applied B3LYP to determine the structure of a molecule and then carried out a single-point calculation by using the wB97X-D functional to evaluate the corresponding frontier orbitals from TD-DFT.

It is noted that the TD-DFT calculations in this work were done under the assumption that the conformation for the DFT geometry optimization is a stable one. By using the same conformation for both DFT and TD-DFT, a direct comparison can be done between the above two computational methods on their predictions of frontier orbitals. As discussed in the previous paragraph, aniline was chosen, as an example, to test the feasibility of the assumption. First, the stable aniline conformation was obtained from the B3LYP with the 6-311++g(d,p) basis set through geometry optimization. This conformation was then entered into ωB97X-D3 for the geometry optimization calculation again. The calculated bond lengths, bond angles, and dihedral angles differed by less than 1% between the two methods. Such a test supported our choice to perform a single-point calculation in the ωB97X-D3-based TD-DFT. Meanwhile, the assumption deserves a more systematic investigation in the future.

Hückel theory and its modified version

For the benzene derivatives investigated here, the π electrons around the benzene ring can be depicted by a 6 x 6 Secular determinant under the Hückel approximations[13,14], with a minor modification, given below.

$$\begin{bmatrix} \alpha_1 - E & \beta_1 & 0 & 0 & 0 & \beta_1 \\ \beta_1 & \alpha - E & \beta & 0 & 0 & 0 \\ 0 & \beta & \alpha - E & \beta & 0 & 0 \\ 0 & 0 & \beta & \alpha - E & \beta & 0 \\ 0 & 0 & 0 & \beta & \alpha - E & \beta \\ \beta_1 & 0 & 0 & 0 & \beta & \alpha - E \end{bmatrix} = 0 \qquad (1)$$

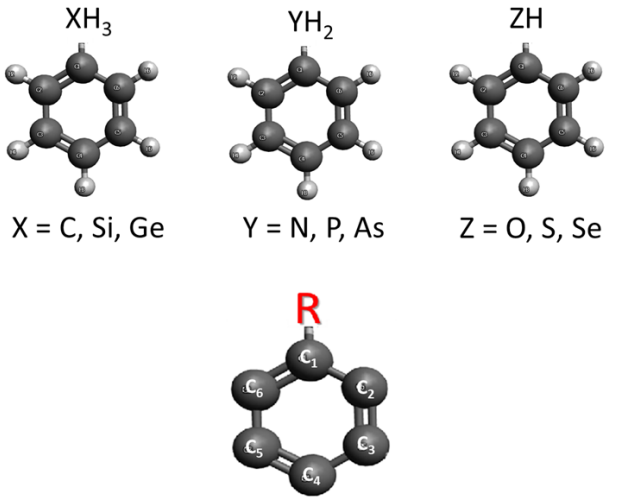

Figure 1. The molecule of benzene derivatives and a simplified Hückel model studied in this work where R denotes the substituent group.

where E is the energy of a molecular orbital; α_1 is the Coulomb integral for the carbon (C_1 in Figure 1) bound to the substituent group; β_1 is the Resonance integral between the carbon atom (C_2 or C_6 in Figure 1) and C_1; α and β are the Coulomb integral and the Resonance integral for the rest of the carbon atoms, respectively. Equation (1) considers a more general scenario where α_1 and β_1 accounts for electrons around C_1 being perturbed by the bound substituent group, like the C_1 of aniline, in Figure 1, and such a perturbation propagates to the adjacent carbon atoms (C_2 and C_6) next to C_1.

Equation (1) can be expanded to the following form:

$$[E-(\alpha+\beta)]\,[E-(\alpha-\beta)]\{E^4 + (-3\alpha - \alpha_1)\,E^3 + (3\alpha^2 + 3\alpha\alpha_1 - 3\beta^2 - 2\beta_1^2)E^2 + [-\alpha^3 - 3\alpha^2\alpha_1 + (3\beta^2 + 4\beta_1^2\alpha + 3\alpha_1\beta^2)]E + \alpha^3\alpha_1 - 2\alpha^2\beta_1^2 - 3\alpha\alpha_1\beta^2 + 4\beta^2\beta_1^2\} = 0 \qquad (2)$$

It is noted that the expressions of the two eigenenergies: $E = \alpha + \beta$ and $E = \alpha - \beta$ in Equation (2) are same as the HOMO and LUMO energy expressions, respectively, in benzene from Hückel theory. But, $E = \alpha + \beta$ and $E = \alpha - \beta$ may not be the HOMO and/or LUMO states in benzene derivatives. When $\alpha_1 = \alpha$ and $\beta_1 = \beta$, the model in Equation (1) is reduced to a homonuclear conjugate six-member ring, like benzene. Note that such a model has been widely applied to investigate heteronuclear benzene rings, such as pyridine.[13] Here, this model was extended to compare with the quantum calculation results. In the following, the value of α (= -11.0×10² kJ/mol) identical to that in benzene will be used[18] to study how each derivative would deviate from benzene.

Results and discussion

The optimized molecular geometries predicted by DFT were summarized in Figure 2, along with the bond length between the substituent atom and the adjacent carbon on the benzene ring, the bond angle centered at the main atom in the substituent group, and

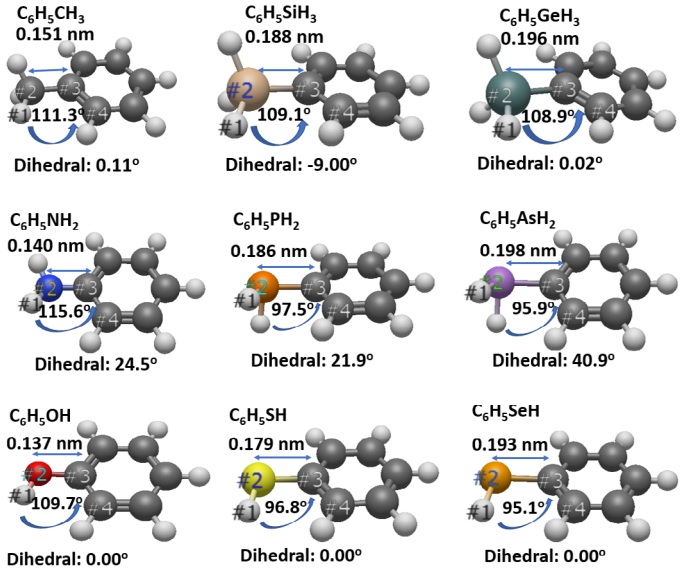

Figure 2. Optimized molecular geometries of all benzene derivatives predicted by DFT together with the bond distance between the substituent element and the closest carbon atom, the bond angle centered at the substituent element, and the dihedral angle marked on each molecule.

the dihedral angle marked on the structure for each compound. The structure of the benzene ring in all derivatives remains the same as an isolated benzene. The dihedral angles of the three C_6H_5-ZH compounds are basically the same in Figure 2 with the -ZH group lying on the same plane as the benzene ring. For C_6H_5-XH_3, their dihedral angles have minor fluctuations, and in C_6H_5-YH_2, the dihedral angle of C_6H_5-AsH_2 in Figure 2 deviates more from the other two compounds.

Figure 3 compares the HOMO-1, HOMO, LUMO, and LUMO+1 energy among different substituent groups between TD-DFT and DFT. The two methods predict similar trends on molecular orbitals for each group, but their energy values are quite different for a given orbital. For different groups, both methods show different trends.

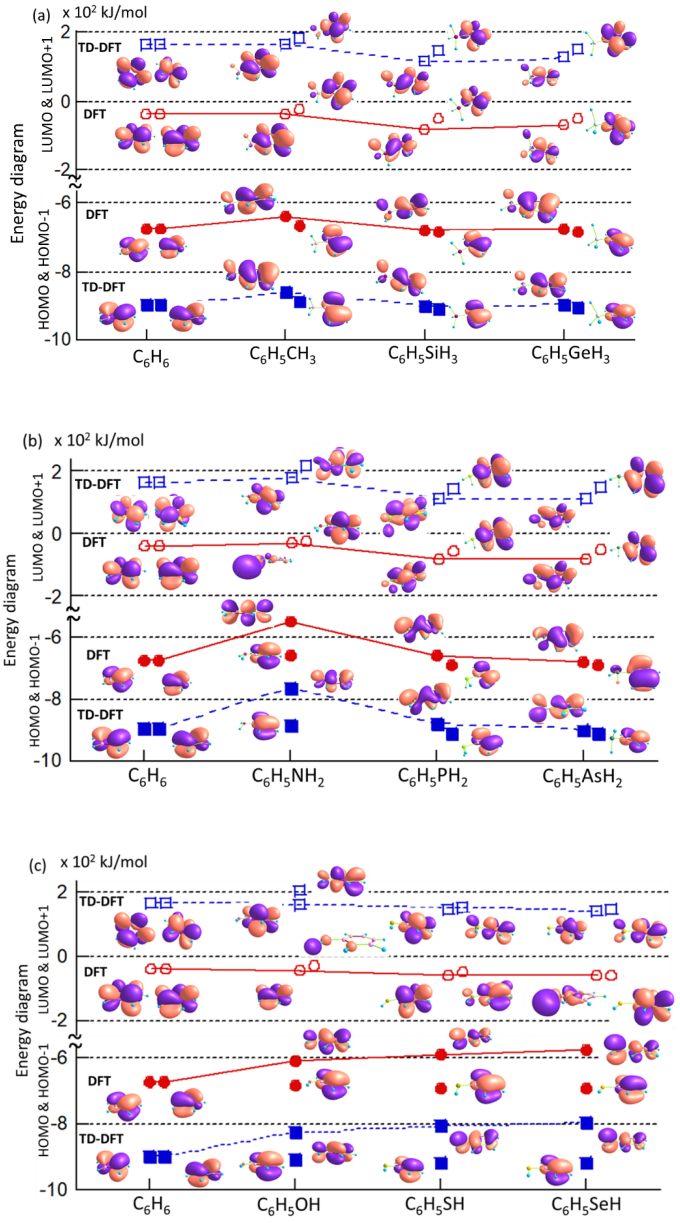

Figure 3. Compare HOMO-1(solid symbols), HOMO (solid symbols), LUMO (open symbols), and LUMO+1 (open symbols) between DFT (denoted by circles) and TD-DFT (denoted by squares) for C_6H_5-XH_3 where X = C, Si and Ge in (a); for C_6H_5-YH_2 where X = N, P, and As in (b); and for C_6H_5-ZH where Z = O, S and Se in (c) together with benzene. Note that when two symbols overlap, they are placed horizontally. Lines are meant for eye guide.

Figure 4 plots the HOMO-LUMO gaps (ΔE(LUMO-HOMO) = E(LUMO) – E(HOMO)) as a function of benzene derivatives, including benzene, based on the period of the non-hydrogen element on the periodic table in a substituent group. As expected, all the substituent groups induce red shifts for their derivatives in contrast to benzene in Figure 4. Actually, both TD-DFT and DFT predict that the energy difference between LUMO and LUMO+1 is smaller as opposed to the difference between HOMO and HOMO-1 due to the electron-donating nature of substituent groups. But the TD-DFT finds a higher LUMO energy and a lower HOMO energy, respectively, compared to the DFT for a given derivative.

Figure 5 displays ΔE(LUMO-HOMO) from both TD-DFT and DFT calculations as a function of the (Pauling scale) electronegativity[19] difference ($\chi - \chi_{carbon}$) between the main element of the substituent group and the carbon for all the benzene derivatives as well as benzene. The statistical correlations from linear regression between ΔE(LUMO-HOMO) and $\chi - \chi_{carbon}$ are found around 0.56 for both DFT and TD-DFT, indicating an intermediate correlation between the HOMO-LUMO gap and the electronegativity of the

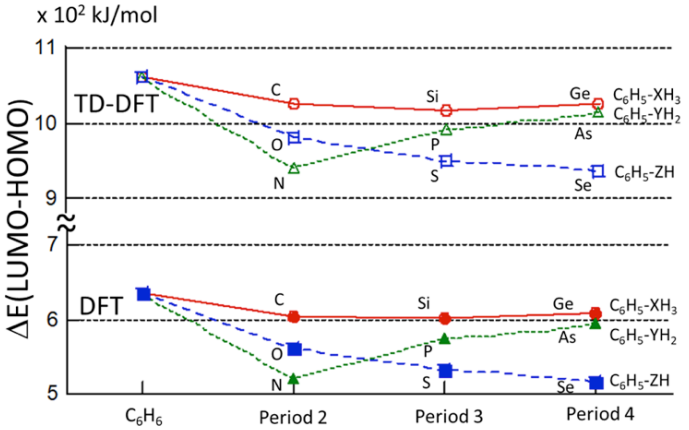

Figure 4. Compare the effect of the elements, as marked, from the benzene substituents on the HOMO-LUMO energy gap (ΔE (HOMO-LUMO) calculated from DFT (solid symbols) and TD-DFT (open symbols)). Lines are meant for eye guide.

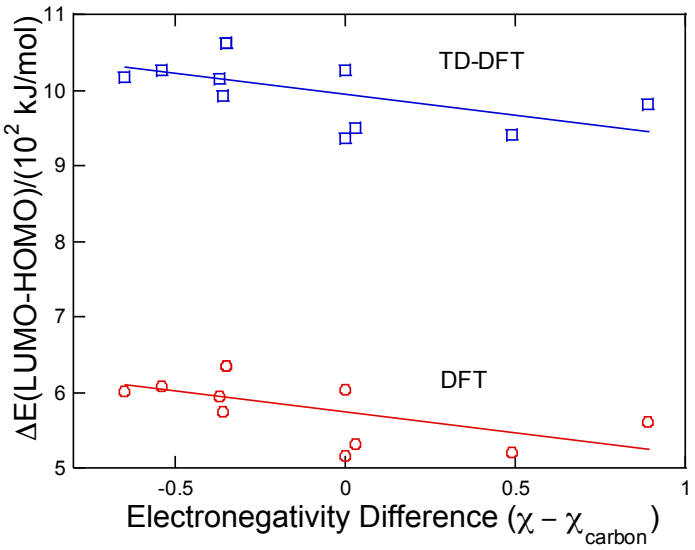

Figure 5. ΔE (LUMO-HOMO) is plotted against the electronegativity difference ($\chi - \chi_{carbon}$) between the main element in the substituent group and the carbon for DFT and TD-DFT, as marked. The statistical correlation from linear regression between ΔE (HOMO-LUMO) and $\chi - \chi_{carbon}$ is found about 0.56 for both DFT and TD-DFT.

non-hydrogen element in a substituent. These results suggest that the electronegativity of the element in the substituent is a factor responsible for the observed trends in Figure 5.

Besides the ΔE(LUMO-HOMO) trends observed in Figures 4 and 5, the fundamental differences between DFT and TD-DFT were differentiated by using Hückel theory. First, in Hückel theory, the HOMO and LUMO energy of benzene are given by $\alpha + \beta$ and $\alpha - \beta$, respectively. To quantitatively compare DFT and TD-DFT with Hückel theory, one needs the reference zero energy in DFT and TD-DFT.

Supposed E^o(DFT) (or E^o(TD-DFT)) is the difference between the reference zero energy between DFT (or TD-DFT) and Hückel theory. Then, E_{DFT}(HOMO) + E^o(DFT) = $\alpha + \beta$ and E_{DFT}(LUMO) + E^o(DFT) = $\alpha - \beta$ for DFT. By the same token, $E_{TD\text{-}DFT}$(HOMO) + E^o(TD-DFT) = $\alpha + \beta$ and $E_{TD\text{-}DFT}$(LUMO) + E^o(TD-DFT) = $\alpha - \beta$ for TD-DFT. In the case of benzene, E_{DFT}(HOMO) = -6.7420×10^2 kJ/mol and E_{DFT}(LUMO) = -0.3823×10^2 kJ/mol. Therefore, E^o(DFT) = -7.44×10^2 kJ/mol and $\beta = -3.18\times10^2$ kJ/mol by knowing $\alpha = -11.0\times10^2$ kJ/mol for benzene.[18] Similarly, with $E_{TD\text{-}DFT}$(HOMO) = -8.9554×10^2 kJ/mol and $E_{TD\text{-}DFT}$(LUMO) = -1.6606×10^2 kJ/mol, E^o(TD-DFT) = -7.35×10^2 kJ/mol and $\beta = -5.31\times10^2$ kJ/mol. Based on these calculations, both DFT and TD-DFT have a similar reference zero energy. The difference between DFT and TD-DFT mainly lies in their ways of computing resonance integrals.

Noticeably, for $C_6H_5NH_2$ and C_6H_5SeH, DFT predicts that their LUMO levels in Figure 3 are primarily composed of the atomic orbitals from the substituent groups, other than having a significant contribution from the π orbitals of the benzene ring. The above result is inconsistent with the predictions of other derivatives in the same group. Besides, from the previous study of aniline by Drougasa et al [20], it is clear that such a LUMO orbital from DFT is ambiguous. On the contrary, all LUMO states calculated from TD-DFT resemble the benzene-like π orbitals and are physically more feasible to further our studies of the HOMO and LUMO states of benzene derivatives.

Table 1 investigates how α_1 and β_1 affect the the frontier orbital energies of Hückel theory in Equation (1). First, the solutions ($\alpha + \beta$ and $\alpha - \beta$) remain as two out of six solutions in Equation (1), which are the Hückel energies for the HOMO and LUMO of benzene, respectively. When $\beta_1 = -5.79 \times 10^2$ kJ/mol, the HOMO and LUMO energy levels stay as $\alpha + \beta$ and $\alpha - \beta$, respectively. As β_1 is adjusted to -5.02×10^2 kJ/mol, the HOMO energy is above $\alpha + \beta$. For $\beta_1 = -4.82 \times 10^2$ kJ/mol and -4.43×10^2 kJ/mol, the HOMO and LUMO fall in-between $\alpha + \beta$ and $\alpha - \beta$. Namely, by adjusting α_1 and β_1, $\alpha + \beta$ and $\alpha - \beta$ can be in the states that are not of HOMO and LUMO energies. Most importantly, the HOMO and LUMO energy levels change altogether, similar to the trends observed in the DFT and TD-DFT calculations.

Table 1. Dependence of α_1 and β_1 on the HOMO and LUMO energy level of Hückel theory

α_1 (x 10^2 kJ/mol)	β_1 (x10^2 kJ/mol)	HOMO-1 (x 10^2 kJ/mol)	HOMO (x 10^2 kJ/mol)	LUMO (x 10^2 kJ/mol)	LUMO+1 (x 10^2 kJ/mol)
-10.4	-5.79	-16.4	-16.3 (=α + β)	-5.69 (=α - β)	-5.22
-10.4	-5.02	-16.3 (=α + β)	-15.9	-5.69 (=α - β)	-5.69
-10.4	-4.82	-16.3 (=α + β)	-15.8	-5.82	-5.69 (=α - β)
-10.4	-4.34	-16.3 (=α + β)	-15.4	-6.19	-5.69 (=α - β)

Note that all the energies are in the unit of (x 10^2 kJ/mol) and are calculated based on Equation (1) where $\alpha_1 = -10.4$ x 10^2 kJ/mol, $\alpha = -11.0$ x 10^2 kJ/mol and $\beta = -5.31$ x 10^2 kJ/mol.

Following the above scheme, Hückel theory was applied to fit the benzene derivative series C_6H_5ZH and $C_6H_5CH_3$. Table 2 summarizes the result of fitting. The parameters α_1 and β_1 for each compound that fits the HOMO and LUMO energies from TD-DFT were identified. In C_6H_5ZH, their HOMO levels increase and LUMO levels decrease as the element Z moves down the group. Meanwhile, the HOMO and LUMO energies of any C_6H_5ZH derivative and $C_6H_5CH_3$ lie in-between those of benzene (namely, between $\alpha + \beta$ and $\alpha - \beta$). Note that the energies listed in parentheses in Table 2 were obtained from TD-DFT. For the rest of the derivatives in Figure 1, their HOMO and LUMO energies are above $\alpha + \beta$ or below $\alpha - \beta$, and cannot be fitted by this method.

Figure 6 plots the α_1/α and β_1/β based on the fitting parameters in Table 2 for the C_6H_5ZH series against the period where each Z-atom is located in the periodic table. The fitting parameters exhibit general trends: α_1 is near the same for all three compounds with $|\alpha_1| < |\alpha|$. Also, the magnitude of β_1 decreases when the element moves down the group, and $|\beta_1| < |\beta|$ for all three cases. The findings may suggest that the substituents in the C_6H_5ZH series tend to donate electrons to the benzene ring, which increases the chance for electrons to distribute around the benzene ring along with an increase of repulsion. As such, both α_1/α and β_1/β are less than one (compared to those in benzene). The near constant

Table 2. The parameters α_1 and β_1 in Hückel theory that fit with the TD-DFT results.

	α_1 (× 10^2 kJ/mol)	β_1 (× 10^2 kJ/mol)	$E_{TD\text{-}DFT}$ (HOMO) + E^o(TD-DFT) (× 10^2 kJ/mol)	$E_{TD\text{-}DFT}$ (LUMO) + E^o(TD-DFT) (× 10^2 kJ/mol)
C_6H_5OH	-10.11	-4.72	-15.56 (-15.58)	-5.77 (-5.77)
C_6H_5SH	-10.18	-4.58	-15.47(-15.42)	-5.91 (-5.91)
C_6H_5SeH	-10.09	-4.50	-15.36 (-15.29)	-5.93 (-5.94)
$C_6H_5CH_3$	-9.94	-5.31	-15.96 (-15.96)	-5.69 (-5.69)

Note that the α_1 and β_1 in Hückel theory are the best fit to the $E_{TD\text{-}DFT}$ (LUMO)+E^o(TD-DFT) from TD-DFT for the benzene derivative series C_6H_5ZH and toluene with $\alpha = -11.0$ x 10^2 kJ/mol and $\beta = -5.31$ x 10^2 kJ/mol. Note that the energy values in parentheses are from TD-DFT.

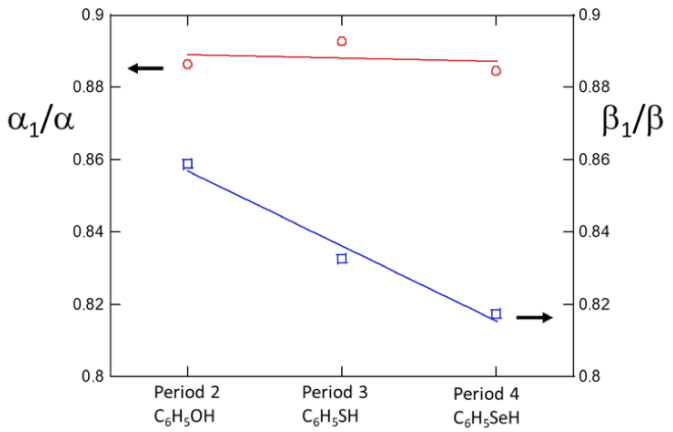

Figure 6. Plot of the α_1/α (denoted by open circles) and β_1/β (denoted by open squares) with α_1 and β_1 obtained from applying the modified Hückel theory to fit the HOMO and LUMO energy data of TD-DFT for the benzene derivative series C_6H_5ZH including Z = O, S, and Se.

α_1 may indicate that the effect of the element Z on carbon C_1 in Figure 1 saturates quickly in the presence of Group 16 elements and becomes insensitive to the actual Z element. Moreover, β_1/β decreases as the element Z moves down the group, which is attributable to the weaker induction effect on a heavier element so that electron-electron repulsions offset the resonance of electrons. Interestingly, the methyl group of toluene impacts the benzene ring locally more on $\alpha_1/\alpha < 1$ than β_1 ($\beta_1/\beta \approx 1$) and will be further discussed later.

The model from Equation (1) represents local corrections on the electron density distortion due to the effect of a substituent group on C_1 and its neighboring bonds (C_1-C_2 and C_1-C_6). For the other two series, $C_6H_5XH_3$ and $C_6H_5YH_2$, their HOMO and LUMO levels do not follow a simple pattern as seen in C_6H_5ZH. The most likely scenario is that the substituent groups in the $C_6H_5XH_3$ and $C_6H_5YH_2$ may have a more global impact on the electron density around the benzene ring. As a result, one may need to use α and β values that are different from those in benzene to quantify their HOMO and LUMO states.

To better address the above point, the correlation of HOMO-1, HOMO, LUMO, and LUMO+1 between benzene and benzene derivatives was analyzed in Figure 7 for C_6H_5-ZH in (a), C_6H_5-YH_2 in (b), and C_6H_5-XH_3 in (c). Figure 2 shows that the -ZH group of C_6H_5-ZH is on the same plane as the benzene ring with a (hybrid) orbital centered at the Z-atom, perpendicular to the plane. In this series, their HOMO and LUMO states are formed by perturbing the degenerate HOMO and LUMO orbitals of benzene. By comparing with TD-DFT, it was found that the two degenerate HOMO (and LUMO) orbitals of benzene are split into two orbitals: HOMO and HOMO-1 (and LUMO and LUMO-1) in a benzene derivative. The HOMO of a C_6H_5ZH has a lower energy than HOMO-1 because the HOMO orbital has no electron density on the C_1 atom of the benzene ring (in Figure 1) and no orbital interaction occurs between the benzene ring and the substituent group. Whereas, in the HOMO-1 orbital, the C_1 atom has an electron density as part of the benzene ring orbital, which induces anti-bonding with the vertical (hybrid) orbital of the substituent group. The formation of a lower-energy LUMO (or a higher-energy LUMO+1) takes the same pattern as HOMO (or HOMO-1).

In the C_6H_5-YH_2 series (Figure 7(b)), the HOMO-1, HOMO, LUMO, and LUMO+1 orbitals of aniline (C_6H_5-NH_2) follow the same trend as those of C_6H_5-ZH, and its two hydrogen atoms are symmetrically located on both sides of the benzene axis, consistent with the work by Drougasa et al.[20] For C_6H_5-PH_2 (or C_6H_5-AsH_2), LUMO and LUMO+1 swap so that LUMO now has a node but LUMO+1 has no node between the P-atom (or As-atom) and C_1. The cause for the lower LUMO orbital with a node is attributed to the orbital from the P-atom (or As-atom) that forms bonding with a lobe in the π^* anti-bonding orbital as shown in Figure 7 (b). The -PH_2 and -AsH_2 groups are located on one side of the benzene main axis that facilitates local bonding formation. The trend of the HOMO and LUMO of the $C_6H_5XH_3$ series in Figure 7 (c) resembles those in $C_6H_5YH_2$. Unlike $C_6H_5PH_2$ and $C_6H_5AsH_2$, the Si and and Ge atoms induce additional bonding by using their d-shaped atomic orbitals to bind with the benzene ring. Noticeably, Si, Ge, P, and As have lower electronegativities than carbon. These elements may release electrons towards the benzene ring and result in a higher electron density around the C_1 atom of benzene near a substituent. Despite the nitrogen atom in -NH_2 having a higher electronegativity than P and As, the strong electron-donating and weaker induction effects of -NH_2 most likely lead to the high HOMO and LUMO energies beyond the limit of Hückel theory.

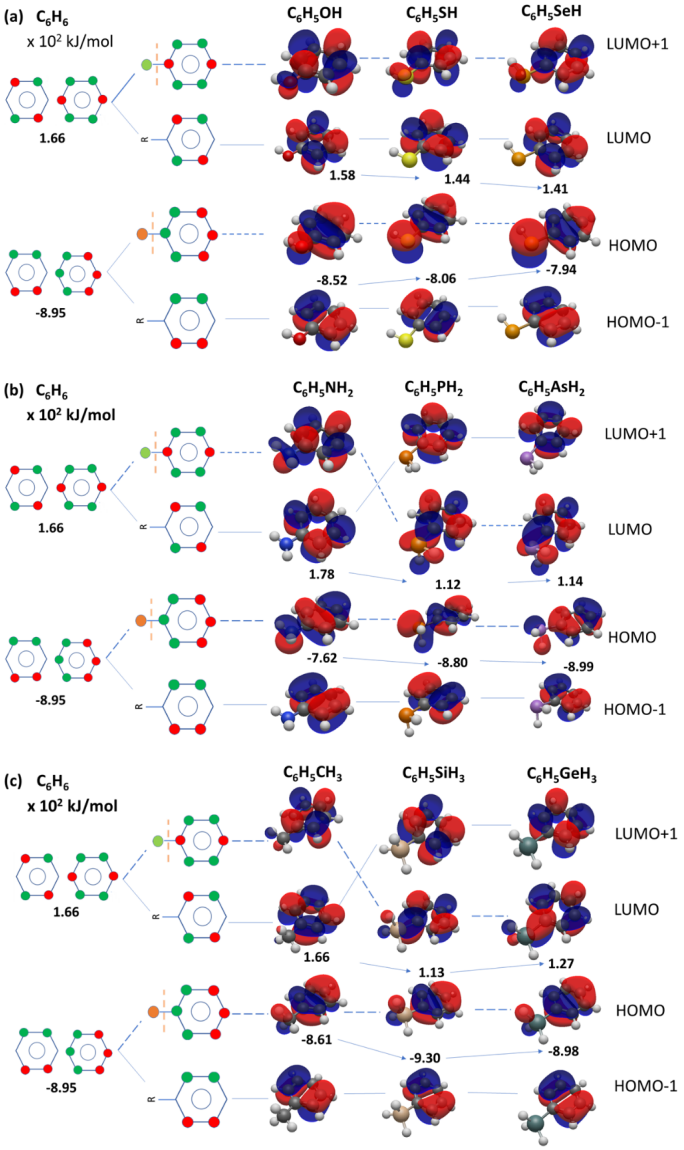

Figure 7. Correlation of HOMO-1, HOMO, LUMO, and LUMO+1 with benzene for the series of C_6H_5ZH in (a), $C_6H_5YH_2$ in (b) and C_6H_5ZH in (c). The energies of HOMO and LUMO of each compound are shown.

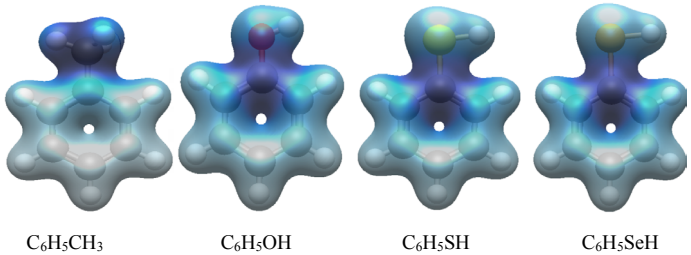

Figure 8. The HOMO electrostatic density of $C_6H_5CH_3$ and the three derivatives of the C_6H_5ZH series from TD-DFT calculations.

Figure 8 compares the electrostatic density map of HOMO between toluene and the three C_6H_5ZH derivatives. The three C_6H_5ZH derivatives exhibit a similar density map with a higher density near C_1 and its neighbors, whereas $C_6H_5CH_3$ has a more significant density localized around the -CH_3 group. The difference is beyond what the electronegativity of the main element in a substituent group can explain. In toluene, the substituent element carbon has the same electronegativity as that of the selenium in benzeneselenol in the Pauling scale.[19] Nevertheless, toluene has a fitting parameter α_1 less negative than that of benzeneselenol in Table 2. Also, the β_1 value of toluene is close to the β value of benzene, but the β_1 value of benzeneselenol tends to be less negative. The non-bonding electrons in -ZH groups could be a factor for the electron donating effect due to resonance structure, for example.[21] The electrostatic density plot in Figure. 8 between these molecules from TD-DFT indicates that a more significant electron density accumulates around the methyl group of toluene that limits the effect of the methyl group on the C_1 atom and maintains a more uniform electron density distribution around its benzene ring with $\beta_1 \approx \beta$. Whereas a higher electron density is found around the C_1 of benzeneselenol suggesting a greater effective attraction between an electron and the C_1 atom that leads to a more negative (attractive) α_1. Since the higher electron density around the C_1 atom increases the repulsion, it causes a less negative (attractive) β_1.

Conclusion

This work investigates the HOMO and LUMO states of three series of benzene derivatives: $C_6H_5XH_3$, X = C, Si, Ge; $C_6H_5YH_2$, Y = N, P, As; and C_6H_5ZH, Z = O, S, Se. The DFT with the chosen functional and basis set predicts reasonable optimized geometries for these compounds. Nevertheless, the LUMO states for some compounds obtained from the DFT can be unphysical. As such, TD-DFT is applied to obtain more physical HOMO and LUMO states. The HOMO-LUMO gaps of these compounds calculated from both methods display similar trends and are correlated to the electronegativity of the element in the substituent groups. Under the framework of Hückel theory, the DFT and TD-DFT were found to differ in their resonance integrals related to electron delocalization energies. Hückel theory was further extended to fit the HOMO and LUMO states of these benzene derivatives. Only those substituent groups that show a good balance between electron-donating and induction, with an element having the electronegativity higher than or similar to a carbon atom, can be quantified. The other substituent groups that form local bonding with the benzene ring or have less induction effect can not be fitted with the simple Hückel theory**.** Our work suggests that these benzene derivatives can be highly valuable for studying the electron-donating and induction effects in the future.

Acknowledgement

CYS thanks partial support from the PSC-CUNY Awards.

References

1. Seeman, J. I.; Tantillo, D. J. ***Chem. Sci.***, **2022**,**13**, 11461-11486.
2. Braga, L. S.; Leal, Daniel H. S.; Kuca, K.; Ramalho, T. C. *Curr. Org. Chem.*, **2020**, 24, 314-331.
3. Kohn, W.; Sham, L. J. *Phys. Rev*. **1965**, 140, A1133 – A1138.
4. Kohn, W.; Becke, A. D.; Parr, R. G. *J. Phys. Chem.* **1996**, 100, 12974-12980.
5. Ziegler, T. *Chem. Rev.* **1991**, 91, 651-667.
6. Runge, E.; Gross, E. K. U. *Phys. Rev. Lett*, **1984**, 52, 997-1000.
7. Zhang, G.; Musgrave, C. B. *J. Phys. Chem. A*, **2007**, 111, 1554-1561.
8. Glebov, E. M.; Fedunov, R. G.; Pozdnyakov, I. P.; Isaeva, E. A.; Zherin, I. I.; Egorov, N. B. *J. Phys. Chem. A*, **2023**, 127, 4704-4714.
9. Wang, X.; Hanif, M. F.; Mahmood, H.; Manzoor, S.; Siddiqui, M. K.; Cancan, M. *Polycyclic Aromatic Compounds*, **2022**, 43, 7754–7768.
10. Aminzai, M.T.; Azizi, N.; Nural, Y.; Yabalak, E. *Monatsh Chem*, **2024**, 155, 115–129
11. M. Mąkosza, *Chem. Eur. J.*, **2020**, *26*, 15346.
12. Atkins P.; de Paula J. and Keeler. J *Physical Chemistry 11th edition* (Oxford University Press, New York 2018 pp. 398-408.
13. Fleming, I. *Molecular Orbitals and Organic Chemical Reactions.* John Wiley & Sons 2010 pp. 32-52
14. Streitwieser, A. *Molecular Orbital Theory for Organic Chemistry.* John Wiley & Sons 1961 pp. 97-134
15. Neese, F. *Interdiscip. Rev.: Comput. Mol. Sci.*, **2012**, 2, 73-78; Neese, F. *Interdiscip. Rev.: Comput. Mol. Sci.,* **2025**, 15, e70019, pp. 1-10.
16. Lakshmishri, S.; Jayavarthanan, T.; Manogaran, K., Sengeny, P.; Venkatachalapathy, V.S.K; Soundhariya, S.; Sivaranjani, T.; Armaković, S. *J. Mol. Liq.*, **2025**, 426, 127361.
17. Tendongmo, H.; Kogge, B. F.; Fouegue, A. D. T; Tasheh, S. N.; Tessa, C. B. N; Ghogomu, J. N. *J. Mol. Model*, **2024** 30, 176.
18. Magnasco, V. *Many-Electron Wavefunctions: Slater, Hartree–Fock and Related Methods, in Elementary Methods of Molecular Quantum Mechanics*, Elsevier Science B.V. 2007 pp. 255-361.
19. Electronegativity data are based on Pauling scale: David R. Lide (ed), *CRC Handbook of Chemistry and Physics, 84th Edition*. CRC Press. Boca Raton, Florida, 2003; Section 9, Molecular Structure and Spectroscopy; Electronegativity; https://en.wikipedia.org/wiki/Electronegativities_of_the_elements_(data_page)
20. Drougasa, E.; Philisb, J. G; Kosmas, A. M. *J. Mol. Struct: THEOCHEM*, **2006**, 758, 17–20.
21. Schore, N.E. and P.C. Vollhardt. *Organic Chemistry, structure and function,* 5th ed. W.H. Freeman and Company (2007) pp. 722-728.